

# Smoothing filters in synthetic cerebral magnetic resonance images: A comparative study

*Filtros suavizadores en imágenes sintéticas de resonancia magnética cerebral: un estudio comparativo*

Elkin Gelvez MSc<sup>1</sup>, <https://orcid.org/0000-0001-5157-3341>, Miguel Vera MSc, PhD<sup>1,2\*</sup>, <https://orcid.org/0000-0001-7167-6356>, Yoleidy Huérfano MSc<sup>2</sup>, <https://orcid.org/0000-0003-0415-6654>, Oscar Valbuena MSc<sup>3</sup>, <https://orcid.org/0000-0003-3080-8839>, Williams Salazar MD<sup>4</sup>, <https://orcid.org/0000-0001-5669-6105>, María Isabel Vera BSc<sup>4</sup>, <https://orcid.org/0000-0003-1135-6283>, Maryury Borrero MSc<sup>1</sup>, <https://orcid.org/0000-0003-3025-1321>, Doris Barrera MSc<sup>1</sup>, <https://orcid.org/0000-0002-6443-6757>, Carlos Hernández MSc<sup>1</sup>, <https://orcid.org/0000-0001-8906-1982>, Ángel Valentín Molina MSc<sup>5</sup>, <https://orcid.org/0000-0001-9604-7222>, Luis Javier Martínez PhD<sup>5</sup>, <https://orcid.org/0000-0003-0917-9847>, Frank Sáenz MSc<sup>6</sup>, <https://orcid.org/0000-0001-9604-7220>, Marisela Vivas MSc, PhD<sup>7</sup>, <https://orcid.org/0000-0002-8941-4562>, Julio Contreras MSc<sup>8</sup>, <https://orcid.org/0000-0002-5179-5400>, Jorge Restrepo PhD<sup>9</sup>, <https://orcid.org/0000-0001-9764-6622>, Juan Vanegas MSc<sup>9</sup>, <https://orcid.org/0000-0003-1955-0195>, Juan Salazar MSc<sup>1</sup>, <https://orcid.org/0000-0001-6826-203X>, Yudith Contreras MSc<sup>1</sup>, <https://orcid.org/0000-0003-4358-730X>.

<sup>1</sup>Universidad Simón Bolívar, Facultad de Ciencias Básicas y Biomédicas, Cúcuta, Colombia.

\*E-mail de correspondencia: m.avera@unisimonbolivar.edu.co

<sup>2</sup>Grupo de Investigación en Procesamiento Computacional de Datos (GIPCD-ULA), Universidad de Los Andes-Táchira, Venezuela.

<sup>3</sup>Grupo de Investigación en Educación Matemática, Matemática y Estadística (EDUMATEST), Facultad de Ciencias Básicas, Universidad de Pamplona.

<sup>4</sup>Servicio de Neurología, Hospital Central de San Cristóbal-Táchira, Venezuela.

<sup>5</sup>Grupo de Investigación en Ingeniería Clínica - HUS (GINIC-HUS), Vicerrectoría de Investigación, Universidad ECCI.

<sup>6</sup>Universidad Simón Bolívar, Facultad de Ingeniería, Cúcuta, Colombia.

<sup>7</sup>Universidad Simón Bolívar, Departamento de Ciencias Sociales y Humanas, Cúcuta, Colombia.

<sup>8</sup>Universidad Simón Bolívar, Facultad de Administración y Negocios, Cúcuta, Colombia.

<sup>9</sup>Grupo de Investigación Research and Enterprise Development (RED), Tecnológico de Antioquia, Medellín, Colombia.

## Abstract

This paper presents the evaluation of two computational techniques for smoothing noise that might be present in synthetic images or numerical phantoms of magnetic resonance (MRI). The images that will serve as the databases (DB) during the course of this evaluation are available freely on the Internet and are reported in specialized literature as synthetic images called BrainWeb. The images that belong to this DB were contaminated with Rician noise, this being the most frequent type of noise in real MRI images. Also, the techniques that are usually considered to minimize the impact of Rician noise on the quality of BrainWeb images are matched with the Gaussian filter (GF) and an anisotropic diffusion filter, based on the gradient of the image (GADF). Each of these filters has 2 parameters that control their operation and, therefore, undergo a rigorous tuning process to identify the optimal values that guarantee the best performance of both the GF and the GADF. The peak of the signal-to-noise ratio (PSNR) and the computation time are considered as key elements to analyze the behavior of each of the filtering techniques applied. The results indicate that: a) both filters generate PSNR values comparable to each other. b) The GF requires a significantly shorter computation time to soften the Rician noise present in the considered DB.

**Keywords:** Synthetic Cerebral images, Magnetic resonance, Rician noise, Gaussian filter, Anisotropic diffusion filter, PSNR.

## Resumen

Este artículo presenta la evaluación de dos técnicas computacionales para el suavizado de ruido, que puede estar presente en imágenes sintéticas o phantoms numéricos de resonancia magnética (MRI). Las imágenes que servirán como bases de datos (DB) para el desarrollo de la mencionada evaluación están disponibles, de manera libre, en la Internet y se reportan, en la literatura especializada, como imágenes sintéticas denominadas BrainWeb. Las imágenes pertenecientes a esta DB fueron contaminadas con ruido Riciano debido a que este es el tipo de ruido más frecuente en imágenes de MRI reales. Por otra parte, las técnicas consideradas para minimizar el impacto de este ruido, en la calidad de las imágenes de la BrainWeb, se hacen coincidir con el filtro Gausiano (GF) y un filtro de difusión anisotrópica, basado en el gradiente de la imagen (GADF). Cada uno de estos filtros posee 2 parámetros que controlan su funcionamiento y, por ende, deben someterse a un proceso de entonación riguroso para identificar los valores óptimos que garanticen el mejor desempeño tanto del GF como del GADF. El pico de la relación señal a ruido (PSNR) y el tiempo de cómputo son considerados como elementos clave para analizar el comportamiento de cada una de las técnicas de filtrado aplicadas. Los resultados indican que: a) Ambos filtros generan valores de PSNR comparables entre sí. b) El GF requiere de un tiempo de cómputo, significativamente, menor para suavizar el ruido Riciano presente en la DB considerada.

**Palabras clave:** Imágenes sintéticas cerebrales, Resonancia magnética, Ruido Riciano, Filtro Gausiano, Filtro de difusión anisotrópica, PSNR.

The magnetic resonance imaging (MRI) databases of real and synthetic data images are affected by a type of noise called Rician noise<sup>1,2</sup>. In MRI, there are several ways to attain the images, called: Proton Density (PD) and relaxation times (T1 and T2). Briefly, it should be pointed out that PD, T1 and T2 consider parameters of the tissues that make up the organ from which the acquisition is intended<sup>1,3</sup>. In that sense, PD represents the concentration of protons in the referred tissues; while T1 and T2 take into account the relaxation times of tissues with a preponderance in a particular direction<sup>2,4</sup>.

Additionally, the mathematical model that governs Rician noise is that of a Rician probability distribution  $P(Z)$ , which is given by equation 1<sup>2</sup>.

$$P(z) = \frac{z}{\sigma^2} e^{-\left(\frac{z+a^2}{2\sigma^2}\right)} I_0 \frac{az}{\sigma^2} \quad (1)$$

Where:  $Z$  is the intensity of the observed voxel ( $A_v$ ),  $a$  is the true intensity value of the  $A_v$ ,  $s$  is the standard deviation of all the values of  $Z$  and  $I_0$  is a Bessel function of first type and zero order.

For the development of this comparative study a synthetic database was considered, called BrainWeb<sup>3,4</sup>, which is available for free downloading on the Internet, at the address <http://brainweb.bic.mni.mcgill.ca/brainweb/>. Images of this BrainWeb base have as a particular characteristic to be contaminated with Rician noise and that was the reason why it was selected as a synthetic reference database for the present work. The features of BrainWeb are described in the next section<sup>5</sup>.

### Description of the databases used: Base BrainWeb

The BrainWeb database (DB) aims to contribute to the validation of techniques that allow the analysis of data from medical images. BrainWeb are images of the human brain generated by a magnetic resonance simulator from a real phantom<sup>6</sup>. The BrainWeb DB consists of:

- Several volumes (3D images) contaminated with different levels of Rician noise.
- A reference volume (ground truth) that is normally used to measure the performance of filtering techniques in response to the Rician noise.

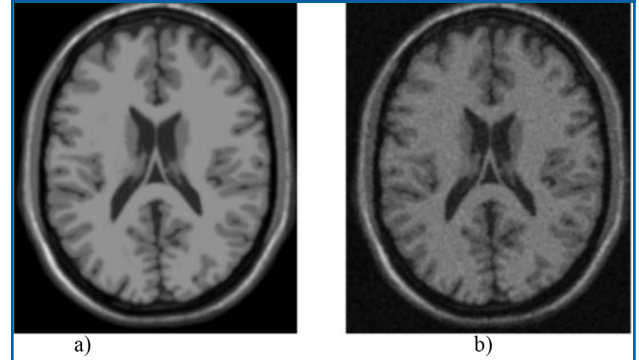
For example, if the acquisition is made with the T1 mode and brain images containing 8-bit unsigned integer the level gray levels are generated, according to Coupé et al.<sup>7</sup>, the mean of the brightest tissue intensity is 150. In this DB, the noise is expressed as a percentage of the standard deviation of this mean. In this sense, a portion of the

BrainWeb database is composed of volumes contaminated at 1%, 3%, 5%, 7% and 9%. Coupé et al.<sup>7</sup> describe how the process of contamination of the data that make up the BrainWeb database is carried out.

For experimental purposes, the ground truth was selected and a volume acquired through the T1 mode, contaminated with Rician noise at 9%, which is the highest noise level available in BrainWeb. The spatial resolution of the volumes that make up this DB is 181x217x181 voxels.

Figure 1 presents axial views of the information contained in selected images of the BrainWeb database.

Figure 1. Axial views for the BrainWeb database: a) Ground truth or original image without Rician noise. b) Image with Rician noise at 9%.



### Preprocessing

The images that make up the BrainWeb DB, contaminated at 9%, were smoothed by the anisotropic diffusion filters<sup>7,8,9</sup> and Gaussian filters<sup>10,11,12,13</sup>. Since each of the mentioned filters depends on their associated parameters, the application of a process of intonation of such parameters is required. To do this, we experimented with selected parameters from a set of arbitrary ranges<sup>9</sup>. The optimal parameters for each filter were obtained once the validation process was completed.

### Gaussian Filter

The Gaussian filter has been used, traditionally, to eliminate noise in images. This filter can be modeled using equation 2.

$$G(i, j, k) = \frac{1}{(\sqrt{2\pi})^3 \sigma_i \sigma_j \sigma_k} e^{-\left(\frac{i^2}{2\sigma_i^2} + \frac{j^2}{2\sigma_j^2} + \frac{k^2}{2\sigma_k^2}\right)} \quad (2)$$

Where in the expression,  $0 \leq i, j, k \leq (n-1)$ ,  $n$  is the size of the observation window or Gaussian kernel; while  $\sigma_i$ ,  $\sigma_j$  and  $\sigma_k$  represent the standard deviation of each spatial dimension.

There is a compromise between the amount of noise that is eliminated by this filter and the blurring experienced by the image processed by this type of filter. In addition, this blur depends, strongly, on the standard deviation used in the 3D convolution mask of the Gaussian smoothing and the size of said Gaussian mask or kernel. Allowing for this, the standard deviation of the synthetic base subjected to

the filtering process was considered. Additionally, to avoid excessive blurring of the volume to be filtered, 3D masks were selected in sizes (3,3,3), (5,5,5), (7,7,7) and (9,9,9) voxels, that is, a total of 4 filtered versions of the DB contaminated with Rician noise were generated.

### Anisotropic Diffusion Filter, based on the gradient.

Diffusion filters and their discrete implementation, based on the approximation of partial derivatives by means of finite differences, were introduced in the image processing by Perona et al.<sup>8</sup>, with a view to smoothing the information contained within the regions delimited by the edges of an image. Some anisotropic diffusion filters, based on the gradient of the image, can be modeled mathematically by equation 3.

$$\frac{\partial I(x,t)}{\partial t} = \nabla[c(x,t)\nabla I(x,t)]; I(x,0) = I_0(x) \quad (3)$$

Where:  $\nabla I(x,t)$  is the gradient of the image in the voxel  $x$  during time  $t$  and is the partial derivative of  $I(x,t)$  with respect to time and  $c(x,t)$  is given by equation 4.

$$c(x,t) = -\frac{\|\nabla I(x,t)\|}{k^2} \quad (4)$$

### Where $k$ is the conductivity parameter.

As mentioned above in the equations linked to this type of filter, the anisotropic diffusion is based on an edge detector to guide the diffusion process. Normally, these equations are solved numerically using finite differences and by means of an explicit scheme that allows to soften the image in each increment of time, in an iterative way.

However, in the presence of noisy contours, diffusion filters have a tendency to degrade the edges of the images they process in proportion to the number of iterations. For this reason, the number of iterations (Iter) considered was 1, 3, 5 and 7. This range of iterations includes relatively low values which determine that the referred degradation is not excessive.

On the other hand, the parameter  $k$  was varied from 0.1 to 1.1 with a step size of 0.2. For the selection of these values, the work developed in<sup>7</sup> was considered. Taking into account the combination of values selected for Iter and  $k$ , 24 versions were obtained anisotropically smoothed by the synthetic base processed.

### Validation

In order to determine which of the filters exhibits a better performance in the presence of Rician noise present in the BrainWeb database, the so-called signal-to-noise ratio (PSNR) index<sup>14,15</sup> was used. One of the features of the PSNR is that it allows the evaluation of the quality of an image after being subjected to a filtering process. Thus, the higher the PSNR, the better the restoration quality of the filtered image.

The PSNR was calculated using equation 5<sup>15</sup>.

$$PSNR = 20 \log_{10} \frac{GLMax}{RMSE} \quad (5)$$

Where: GLMax is the maximum gray level present in the processed images, RMSE is the square root of the estimated mean square error between the ground truth and the filtered volume.

## Results

### Optimal Parameters

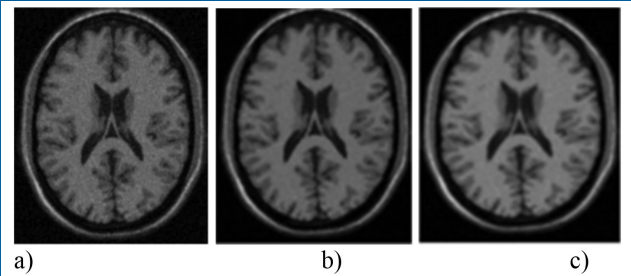
For the anisotropic diffusion filter, the parameters that generated the highest PSNR were: a) Number of Iterations: 3. b) Conductivity: 0.5; while for the Gaussian filter the size of the optimal 3D neighborhood was (3,3,3) voxels.

### Qualitative Results

The selected volume of the BrainWeb base contaminated with Rician noise was filtered, independently, using both the techniques of anisotropic and Gaussian filtering. Because this volume is heavily contaminated, it is possible to visualize easily the Rician noise in any of the axial, coronal or sagittal cuts.

For this reason, only one of them was chosen to present the information related to this type of noise. Thus, figure 2 allows the comparison of the axial view of the polluted volume with the smoothed versions, generated by each of the said filters.

Figure 2. a) Image with Rician noise. b) Anisotropic smoothing. c) Gaussian Filtering.



A visual analysis of these images shows that both the anisotropic filter and the Gaussian smoothing manage to restore, to a large extent, the contaminated image. However, the qualitative analysis of these figures does not allow to establish, without ambiguity, which of the filters exhibits the best behavior; therefore, quantitative results obtained from the calculation of the PSNR are presented which will indicate, precisely, which of the filters delivers the best performance.

### Quantitative Results

The previous qualitative assessment is supported by the data presented in table 1, obtained when calculating the PSNR index for synthetic bases contaminated with Rician noise. This table also shows the computation time used by each filter when processing the selected DB.

Table 1. Performance of the filters with respect to Rician noise, using the PSNR and the computation time required during its application.

Filter	PSNR	Computation Time (Seconds)
Anisotropic	23.72	91.09
Gaussian	23.56	4.56

If the filter-noise ratio is analyzed considering the PSNR values obtained, it can be affirmed that the anisotropic filter obtained the highest value of PSNR, which indicates that it can restore, with a better effectiveness, volumes contaminated with Rician noise.

This may be due, in part, to the fact that this filter uses a scheme based on an edge detector to smooth the image as many times as indicated by the number of iterations, which can be a potential advantage, from the perspective of effectiveness, against the non-iterative scheme on which the Gaussian smoothing is based.

Yet, as reported in the literature and can be seen in Table 1, this effectiveness is achieved through higher computation times than those employed by other smoothing techniques. Additionally, the Gaussian smoothing also has a performance comparable to that of the anisotropic filter. According to what is reported in<sup>7</sup>, Rician noise is strongly linked to Gaussian noise, which partly explains the good performance of the Gaussian filter in the face of Rician noise.

In this context, it is important to point out that, according to the information presented in table 1, the Gaussian filter can perform the smoothing process more quickly than the anisotropic filter; so, in those cases in which the computational cost of the filter favors the Gaussian filter, it can be a good alternative.

In the context of medical images, strictly speaking, it is necessary to develop an intonation process linked to the obtaining of optimal parameters that govern the operation of the filters used in computational processing. This is because it is impossible to know, a priori, the set of parameters that guarantee the best overall performance of the filters when dealing with the problem of noise of any nature and, particularly, Rician noise.

Taking only the PSNR as a reference, there is no doubt that the anisotropic filter exhibits the best performance. The results indicate that the iterative approach complemented with the contour detector on which the anisotropic filter is based turns out to be appropriate when it is intended to minimize the undesirable effects of Rician noise. In fact, according to the values of the optimal parameters for this filter, it is observed that more than one iteration and a low conductance value were required, so that this filter will generate the filtered version with higher PSNR.

If only the computation time is considered as a reference, the Gaussian filter is much more efficient than the anisotropic filter implemented. This is a direct consequence of the iterative approach, of this last filter, requiring more computer resources than the simple scheme on which a Gauss filter is based that applies a direct convolution of the coefficients of its kernel with the gray levels of the

image to soften.

In the context of medical images, it has been demonstrated that the Gauss filter presents excellent attributes and should be one of the main computational smoothing techniques to be considered when facing the problem of Rician noise, the predominant type in both synthetic and real brain MRI images.

According to the results, the choice of the standard deviation of the contaminated synthetic volume as the standard deviation of the Gaussian filter constitutes a good criterion to fix this parameter. As already noted, the standard deviation has a decisive influence on the quality of Gaussian filtering.

### Acknowledgements

The authors are grateful for the financial support given by the Universidad Simón Bolívar-Colombia through the 2016-16 code project.

### References

1. Gudbjartsson H. y Patz S. The rician distribution of noisy MRI data, *Magn. Reson. Med.* 34 (1) (1995) 910914.
2. Macovski A. (1996). Noise in MRI, *Magn. Reson. Med.* 36 (1) 494497.
3. Cocosco C., Kollokian V., Kwan R. y Evans A. (1997). BrainWeb: Online Interface to a 3D MRI Simulated Brain Database. *NeuroImage*, 5(4), part 2/4, S425, 1997. Proceedings of 3-rd International Conference on Functional Mapping of the Human Brain, Copenhagen.
4. Kwan R., Evans A. y Pike G. (1999). MRI simulation-based evaluation of image processing and classification methods. *IEEE Transactions on Medical Imaging*. 18(11):1085-97.
5. Collins D., Zijdenbos A., Kollokian V., Sled J. y Kabani N., Holmes C., Evans A. (1998). Design and Construction of a Realistic Digital Brain Phantom. *IEEE Transactions on Medical Imaging*, 17(3):463-468.
6. Kwan R., Evans A. y Pike G. (1996). An Extensible MRI Simulator for Post-Processing-Evaluation-Visualization in Biomedical Computing (VBC'96). *Lecture Notes in Computer Science*, 1131:135-140. Springer-Verlag,
7. Coupé P., Yger P., Prima S., Hellier P., Kervrann C. y Barillot C. (2008). An optimized blockwise nonlocal means denoising filter for 3-D magnetic resonance images, *IEEE Trans. Med. Imag.* 27(4):425-441.
8. Perona P. y Malik J. (1990). Scalespace and edge detection using anisotropic diffusion, *IEEE Trans. on Patt. Analysis and Machine Intelligence* 12(7): 629-639.
9. Vera M. Segmentación de estructuras cardiacas en imágenes de tomografía computarizada multi-corte. Ph.D. dissertation, Universidad de los Andes, Mérida-Venezuela, 2014.
10. Vera M., Huérfano Y., Contreras J., Vera M. I., Salazar W., Vargas S., Chacón J. y Rodríguez J. (2017). Detección de hemorragia intracranial intraparenquimatosa, en imágenes de tomografía computarizada cerebral, usando una técnica computacional no lineal. *Latinoamericana de Hipertensión*. 12(5), 125-130.
11. Meijering H. Image enhancement in digital X-ray angiography. [Tesis Doctoral], Utrecht University, Netherlands, 2000.
12. González R., Woods R. *Digital Image Processing*. USA: Prentice Hall, 2001.
13. Pratt W. *Digital Image Processing*. USA: John Wiley & Sons Inc, 2007.
14. Netravali A. y Haskell B. *Digital Pictures: Representation, Compression, and Standards (2nd Ed)*, Plenum Press, New York, NY (1995).
15. Rabbani M. y Jones P. *Digital Image Compression Techniques*, Vol TT7, SPIE Optical Engineering Press, Bellvue, Washington (1991).